

Synthesis, Characterisation and Molecular Hyperpolarisabilities of Pseudo-Octahedral Hydrido(nitrile)iron(II) Complexes for Nonlinear Optics: X-ray Structure of $[\text{Fe}(\text{H})(\text{dppe})_2(4\text{-NCC}_6\text{H}_4\text{NO}_2)][\text{PF}_6]\cdot\text{CH}_2\text{Cl}_2$

Maria Paula Robalo,^{*[a,b]} António P. S. Teixeira,^[b,c] Maria Helena Garcia,^[b,d]
M. Fátima Minas da Piedade,^[b,d] M. Teresa Duarte,^[b] Alberto Romão Dias,^[b]
Jochen Campo,^[e] Wim Wenseleers,^{*[e]} and Etienne Goovaerts^[e]

Keywords: Hydride ligands / Iron / Nonlinear optics / Hyperpolarizability / Hyper-Rayleigh scattering

A series of ionic pseudo-octahedral *trans*-hydrido(nitrile)-iron(II) complexes with the general formula $[\text{Fe}(\text{H})(\text{dppe})_2(4\text{-NCR})][\text{PF}_6]$ [dppe = 1,2-bis(diphenylphosphanyl)ethane; R = acceptor-substituted conjugated ligand] have been synthesised by chloride abstraction from the starting compound *trans*- $[\text{FeHCl}(\text{dppe})_2]$ and fully characterised. First hyperpolarisabilities (β) have been determined by hyper-Rayleigh scattering (HRS) at the fundamental wavelength of 1072 nm and the high near-resonant values obtained (up to 1130×10^{-30} esu) are interpreted in terms of the two-level model (TLM) and are correlated with IR and NMR spectroscopic data. Wavelength-dependent HRS has been performed in the

1072–1580 nm range for two of the compounds, namely $[\text{Fe}(\text{H})(\text{dppe})_2\{4\text{-NC}(\text{CH})(\text{CH})\text{C}_6\text{H}_4\text{NO}_2\}][\text{PF}_6]$ and $[\text{Fe}(\text{H})(\text{dppe})_2\{4\text{-NCC}_6\text{H}_4(\text{CH})(\text{CH})\text{C}_6\text{H}_4\text{NO}_2\}][\text{PF}_6]$. These results clearly show the two-photon resonance but also the shortcomings of the TLM when it comes to deriving reliable static β values. A structural study of the compound $[\text{Fe}(\text{H})(\text{dppe})_2(4\text{-NCC}_6\text{H}_4\text{NO}_2)][\text{PF}_6]$ by X-ray diffraction shows that it crystallises in the centrosymmetric monoclinic space group $P2_1/n$, with four molecules in the unit cell and a pairwise antiparallel alignment of the dipoles.

(© Wiley-VCH Verlag GmbH & Co. KGaA, 69451 Weinheim, Germany, 2006)

Introduction

Organometallic molecules have been extensively studied in the search for new materials with enhanced second-order nonlinear optical (NLO) properties.^[1–7] Because of their large first hyperpolarisabilities (β), fast response times and architectural flexibility, they have many potential applications in photonic devices such as frequency doublers, photonic switches and electro-optic modulators.^[8] Many studies have focused on organic and organometallic molecules composed of a highly polarisable π -conjugated backbone with an electron-donor (D) and an -acceptor (A) group attached to opposite ends. In this way a so called asymmetric

“push-pull” or D- π -A system is created, which can be used to obtain a macroscopically non-centrosymmetric medium with a large second-order nonlinear susceptibility.^[3] In the search for better donor and acceptor groups, it appeared that an organometallic moiety could serve as a very efficient alternative electron-donor group to the traditional, purely organic, push-pull system.^[1,2,5–7,9] In these systems, the characteristic charge transfer from metal to ligand (MLCT) could be the origin of a large charge separation over the long conjugated ligand, which can be tuned to optimise the molecular nonlinear optical properties. We have previously reported hyper-Rayleigh scattering (HRS) results for such a systematically varied series of ionic organometallic complexes, consisting of a transition metal centre coordinated by an η^5 -monocyclopentadienyl ring, a bidentate phosphane ligand and a conjugated nitrile ligand.^[10–12] By comparing complexes with electron-donor and -acceptor substituted ligands we found that the ruthenium and especially the iron fragments could be used as very efficient electron-donor groups.

In order to further enhance the NLO response new structural changes are now implemented. First of all, the donor fragment is modified by replacing the η^5 -monocyclopentadienyl ring by a second bidentate phosphane ligand [1,2-bis(diphenylphosphanyl)ethane, $\text{Ph}_2\text{P}(\text{CH}_2)_2\text{PPh}_2$, dppe] and a hydride, which leads to a pseudo-octahedral coordi-

[a] Departamento de Engenharia Química, Instituto Superior de Engenharia de Lisboa,
Rua Conselheiro Emídio Navarro, 1, 1950-062 Lisboa, Portugal
Fax: +351-21-831-7267
E-mail: mprobalo@deq.isel.ipl.pt

[b] Centro de Química Estrutural, Instituto Superior Técnico,
Av. Rovisco Pais, 1049-001 Lisboa, Portugal

[c] Departamento de Química, Universidade de Évora,
Colégio Luís A. Verney, Rua Romão Ramalho, 59, 7000-671 Évora, Portugal

[d] Faculdade de Ciências da Universidade de Lisboa, Campo Grande,
Edifício C8, 1749-016 Lisboa, Portugal

[e] Department of Physics, University of Antwerp, Campus Drie Eiken,
Universiteitsplein 1, 2610 Wilrijk-Antwerpen, Belgium
E-mail: wim.wenseleers@ua.ac.be

nation at the transition metal. This coordination creates new possibilities for fine-tuning the molecular structure since an extra ligand can be bound to the metal *trans* to the conjugated ligand. Because of the pseudo-octahedral coordination it also becomes possible to use these complexes as a building block for highly branched macromolecules or metallodendrimers,^[13,14] which have promising applications in nonlinear optics. A series of pseudo-octahedral ruthenium acetylide compounds^[15] exhibits even higher β values^[16] than the analogous cyclopentadienyl compounds studied before,^[17] although they are about equally resonant. Therefore, in this work, the favourable iron centre is combined with the pseudo-octahedral surrounding and with a nitrile linkage in order to obtain very high hyperpolarisabilities together with extensive molecular versatility. Apart from the improvement of the metallic electron donor, we have also looked for a more efficient acceptor by introducing a second nitro group at the conjugated backbone. Finally, the conjugated backbone itself, which connects the electron-acceptor and -donor groups, is also varied in both length and structure to further optimise the hyperpolarisability.

Results and Discussion

Preparation of the Pseudo-Octahedral Iron(II) Dppe Derivatives

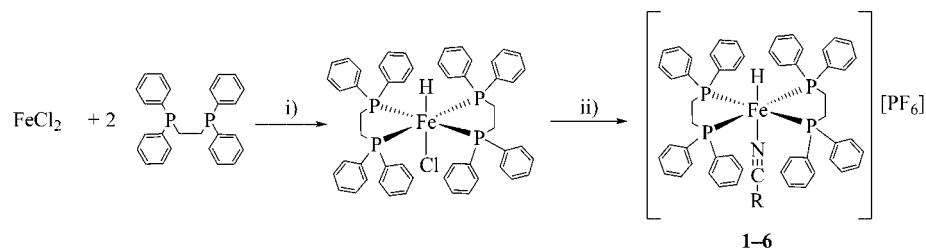
The complexes of general formula $[\text{Fe}(\text{H})(\text{dppe})_2(4\text{-NCR})][\text{PF}_6]$ were prepared following a general procedure that involves chloride abstraction from the starting compound *trans*- $[\text{FeHCl}(\text{dppe})_2]$ by TIPF_6 , in the presence of a slight excess of the corresponding nitrile chromophores (see Scheme 1). The reactions were carried out in CH_2Cl_2 or

THF by stirring at room temperature for several hours. After work-up, the compounds were obtained in moderate to high yields (37–71%).

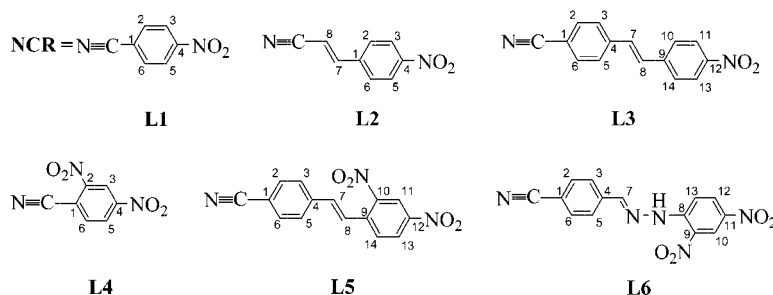
Characterisation of the New Complexes $[\text{Fe}(\text{H})(\text{dppe})_2(4\text{-NCR})][\text{PF}_6]$

All of the *trans*-hydrido(nitrile)iron(II) complexes were obtained as deep-red or purple crystals with the exception of $[\text{Fe}(\text{H})(\text{dppe})_2(2,4\text{-NCC}_6\text{H}_3(\text{NO}_2)_2)][\text{PF}_6]$ (**4**), which is dark green. They are fairly air stable in the solid state towards oxidation, but less stable in solution. They are soluble in polar solvents and insoluble in less polar and apolar organic solvents. The complexes were characterised by a combination of IR and ^1H , ^{13}C and ^{31}P NMR spectroscopy, and elemental analysis.

The solid-state IR spectra (KBr pellets) of complexes **1–6** present a large number of bands due to the presence of the various co-ligands. They exhibit strong $\nu(\text{NC})$ bands in the range $2138\text{--}2185\text{ cm}^{-1}$ (see Table 1) at lower wavenumbers than those observed for the corresponding uncoordinated nitriles. Thus, on coordination of the nitrile to the metal fragment, the NC stretching band shifts by 33 to 101 cm^{-1} to lower frequency. This weakening of the NC bond is consistent with a π back-donation interaction $d_{\pi}(\text{Fe})\text{--}\pi^*(\text{NC})$, which makes the metal group a more effective donor. This shift is found to be much higher in the present complexes than in the cyclopentadienyl compounds,^[10] where shifts of up to 35 cm^{-1} were obtained. The π back-donation is enhanced by the interaction between the electron-donating metal moiety and the electron-accepting nitro group through the conjugated chain, as desired for a large first hyperpolarisability. In agreement with this in-



i) NaBH_4 , $T = 60\text{ }^\circ\text{C}$, 2 h, ethanol; ii) exc. NCR, TIPF_6 , CH_2Cl_2 or THF, r.t. 2–18 h



Scheme 1. Synthesis of complexes **1–6** (showing the numbering scheme for NMR spectral assignments).

Table 1. The experimental hyperpolarisabilities, β_{zzz} , measured by HRS at $\lambda = 1072$ nm in chloroform, together with optical and spectroscopic data. λ_{\max} is the spectral position of the lowest energy transition; ϵ_{\max} is the corresponding extinction coefficient.

Complexes	Pseudo-octahedral compounds [Fe(H)(dppe) ₂ (<i>p</i> -NC-R)] ⁺ [PF ₆] ⁻ (for R see Scheme 1)						η^5 -Monocyclopentadienyl compounds ^[12]	
	1	2	3	4	5	6	7 (<i>p</i> -NC-R = L1)	8 (<i>p</i> -NC-R = L2)
λ_{\max} (nm)	546	549	485	723	505	503	460	484
ϵ_{\max} (L mol ⁻¹ cm ⁻¹)	7700	8800	8300	8300	10300	10700	6000	8700
$\beta_{\text{complex}}^{zzz}$ (10 ⁻³⁰ esu)	700	860	800	435	1130	1026	395 ^[a]	570 ^[a]
$\beta_{\text{ligand}}^{zzz}$ (10 ⁻³⁰ esu)	4.4 ^[a,b]	–	33	5.6	41	47	–	–
$\nu(\text{C}\equiv\text{N})^{[c]}$ (cm ⁻¹)	2177	2174	2185	2138	2182	2183	2205	2205
$\Delta\nu(\text{C}\equiv\text{N})^{[c]}$ (cm ⁻¹)	-56	-43	-33	-101	-40	-39	-35	-15
$\nu(\text{Fe-H})^{[c]}$ (cm ⁻¹)	1870	1853	1888	1891	1891	1896	–	–
$\delta(^1\text{H}_{\text{hydride}})^{[d]}$ (ppm)	-17.48	-18.03	-18.83	-14.60	-18.67	-18.54	–	–
$\delta(^1\text{H}_{\text{ar}})^{[d]*}$ (ppm)	6.73	5.65	6.76	5.43	6.77	6.79	6.97 ^[e]	5.95 ^[e]
$\Delta\delta(^1\text{H}_{\text{ar}})^{[d]}$ (ppm)	-1.17	-0.43	-0.94	-2.78	-0.96	-1.11	-1.16 ^[e]	-0.64 ^[e]
$\delta(^{31}\text{P}_{\text{dppe}})^{[d]}$ (ppm)	83.34	83.80	83.74	81.00	83.48	83.45	98.09 ^[f]	97.64 ^[f]

[a] At 1064 nm. [b] In methanol.^[10] [c] KBr pellets, some bands are very weak. [d] CD₂Cl₂, room temperature. [e] (CD₃)₂CO, room temperature. [f] CDCl₃, room temperature; * H adjacent to NC group.

terpretation, the shifts are dependent on the number of nitro groups present at the nitrile ligand and on the distance between the NC and NO₂ groups. Thus, the highest shift is found for **4** due to the presence of two strongly electron-withdrawing nitro groups separated by only a short, well-conjugated link from the donor group. The trend in the values indicates that removal of electron density from the nitrile linkage becomes less marked on chain lengthening. For the dinitro derivatives (compounds **5** and **6**), the position of the $\nu(\text{NC})$ absorption seems to be independent of the type of conjugated bridge between the aromatic rings. The $\nu(\text{Fe-H})$ bands are very weak, with high frequencies in the range 1853–1896 cm⁻¹, consistent with a strongly bound hydride *trans* to an aromatic nitrile.^[18,19]

The ¹H NMR spectra of the compounds were obtained in CD₂Cl₂ solutions. The chemical shifts of the dppe protons are within the range of other octahedral iron(II) complexes with coordinated nitriles and are almost constant in all compounds synthesised. The hydride is observed upfield of the TMS signal ($\delta = -14.6$ to -18.8 ppm) (see Table 1) as a quintuplet due to coupling with the phosphorus atoms of the dppe units, thus showing that all phosphorus atoms are equivalent, in an equatorial position, with a *trans* orientation between the hydride and the nitrile ligands. The position of the hydride signal is affected by the nitrile ligand and it also seems to be dependent on the distance between the NC and NO₂ groups, with short distances changing the signal to less-negative chemical shifts. This observation is consistent with a hydride ligand coordinated *trans* to a good π -acceptor like the nitrile ligands, as reported before.^[20] Upon coordination of the nitrile ligand, the chemical shifts of the aromatic *ortho* protons (relative to the nitrile group) can be used to assess the electron-donating capabilities of the metal centre (see, for instance, refs.^[11,12,21]) and have been shown to be correlated with high molecular hyperpolarisabilities β . An upfield shift of the *ortho* protons, corresponding to a stronger shielding effect, indeed indicates a back-donation from the metal centre to the nitrile ligand and suggests a more efficient donor and/or a stronger acceptor group. For the present complexes all the *ortho* pro-

tons or the H _{β} (in compound **2**) are shielded, with upfield shifts between 0.43 and 2.78 ppm, with the highest shift found for the *ortho* proton of complex **4**. These shifts are much higher than those measured in our previous studies of the cyclopentadienyl compounds (0.05–1.2 ppm),^[11,12,21] which makes the high β values obtained comprehensible (see Table 1).

The compounds were also characterised by ¹³C NMR spectroscopy in [D₂]dichloromethane. The deviations in the chemical shifts of the carbon atoms are small and in agreement with the data observed in the ¹H NMR spectra. The ³¹P{¹H} NMR spectra of these compounds show a single sharp signal in the range $\delta = 81$ –84 ppm, attributed to the phosphorus atoms of the dppe ligand, which confirms that all the complexes adopt an exclusively *trans* configuration in solution. These data are also consistent with the expected deshielding effect upon coordination of the phosphane, since free dppe shows a singlet at $\delta = -12.1$ ppm in the same solvent.

X-ray Structural Determination of [Fe(H)(dppe)₂(4-NCC₆H₄NO₂)] [PF₆] (**1**)

Recrystallisation of compound [Fe(H)(dppe)₂(4-NCC₆H₄NO₂)] [PF₆] (**1**) by slow diffusion of diethyl ether into a dichloromethane solution gave crystals suitable for X-ray diffraction studies. The crystals belong to the monoclinic system (space group *P2₁/n*), with four molecules in the unit cell. The structural studies confirm the presence of I⁺ cations, hexafluorophosphate anions and a crystallisation solvent molecule of dichloromethane. The molecular structure of the cation is shown in Figure 1 (obtained with ORTEP-3^[22]), along with the atom-numbering scheme. Selected bond lengths and angles are given in Table 2.

Complex **1** presents a distorted octahedral coordination geometry with the atoms coordinated to Fe displaying bond angles close to 90° (see Table 2). The X-ray structure confirms the *trans* position of the nitrile and hydride ligands, which define a vertical axis, with the two bidentate phos-

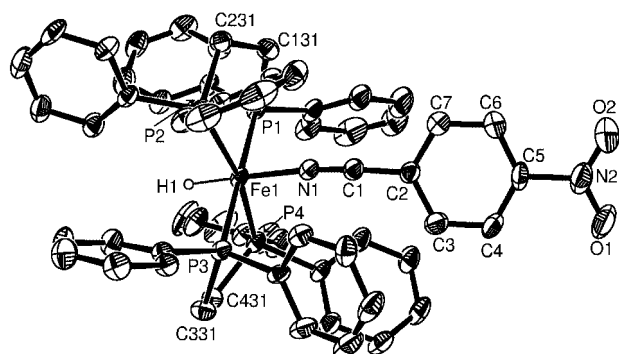


Figure 1. Molecular structure of the cation $[\text{Fe}(\text{H})(\text{dppe})_2(4\text{-NCC}_6\text{H}_4\text{NO}_2)]^+$ with 40% probability thermal ellipsoids, showing the labelling scheme (the hydrogen atoms, except the hydride, have been omitted for clarity).

Table 2. Selected bond lengths [Å], angles [°] and torsion angles [°] for $[\text{Fe}(\text{H})(\text{dppe})_2(4\text{-NCC}_6\text{H}_4\text{NO}_2)][\text{PF}_6]$ (**1**).

Bond lengths [Å]		Angles [°]	
Fe(1)–H(1)	1.45(5)	Fe(1)–N(1)–C(1)	174.2(5)
Fe(1)–N(1)	1.880(5)	N(1)–C(1)–C(2)	175.4(7)
N(1)–C(1)	1.162(7)	C(1)–C(2)–C(3)	119.9(6)
C(1)–C(2)	1.429(8)	C(5)–N(2)–O(1)	118.3(8)
N(2)–C(5)	1.485(9)	C(5)–N(2)–O(2)	117.8(7)
N(2)–O(1)	1.211(9)	O(1)–N(2)–O(2)	123.9(7)
N(2)–O(2)	1.225(9)	H(1)–Fe(1)–P(1)	93(2)
C(Ar)–C(Ar)	1.363–1.388	P(1)–Fe(1)–N(1)	87.78(14)
Fe(1)–P(1)	2.274(2)	H(1)–Fe(1)–P(2)	84(2)
Fe(1)–P(2)	2.256(2)	P(2)–Fe(1)–N(1)	97.57(15)
Fe(1)–P(3)	2.276(2)	H(1)–Fe(1)–P(3)	87(2)
Fe(1)–P(4)	2.226(2)	P(3)–Fe(1)–N(1)	92.37(14)
		H(1)–Fe(1)–P(4)	81(2)
Torsion angles [°]			
Fe(1)–N(1)–C(1)–C(2)	29(11)	P(4)–Fe(1)–N(1)	96.99(15)
N(1)–C(1)–C(2)–C(3)	–38(8)	P(1)–Fe(1)–P(2)	83.15(7)
C(2)–C(7)–C(6)–C(5)	–0.2(12)	P(1)–Fe(1)–P(4)	96.44(7)
C(2)–C(3)–C(4)–C(5)	1.9(11)	P(3)–Fe(1)–P(2)	97.22(7)
C(7)–C(6)–C(5)–N(2)	177.5(7)	P(3)–Fe(1)–P(4)	83.14(7)
C(6)–C(5)–N(2)–O(1)	11.4(8)	P(1)–Fe(1)–P(3)	179.57(8)
C(6)–C(5)–N(2)–O(2)	10.2(11)	P(4)–Fe(1)–P(2)	165.41(7)
C(4)–C(5)–N(2)–O(1)	10.7(10)	H(1)–Fe(1)–N(1)	178(2)
C(4)–C(5)–N(2)–O(2)	9.4(8)		

phane ligands occupying the equatorial plane. The four phosphorus atoms (P1–P4) are roughly coplanar, with an average atomic displacement of 0.1407(6) Å with the Fe atom lying within the plane.

The investigation of the Fe–N and Fe–H bond lengths is of particular interest as they can often indicate the presence

of a d–p π overlap in the Fe–N bond. The hydride could be located and reasonably isotropically refined with an Fe–H bond length of 1.45(5) Å, which is in the lower range of the values observed in similar compounds, as can be seen in Table 3 (hydride structures in refs.^[18–20,23,24]). The Fe–N bond length [1.880(5) Å] is slightly shorter than those observed in these compounds, while the N≡C bond length [1.162(7) Å] is relatively longer (see Table 3). These observations, as well as the Fe(1)–N(1)–C(1) and N(1)–C(1)–C(2) bonding angles of 174.2(5)° and 175.4(7)°, respectively, confirm the existence of Fe→N π back-donation. The distances and angles within the benzonitrile group, in particular the absence of any obvious bond-length alternation, are consistent with the retention of aromaticity. The nitro group is slightly twisted relative to the aromatic ring plane, characterised by $C_{\text{ar}}\text{--}C_{\text{ar}}\text{--}N\text{--}O$ torsion angles of around 10°.

The dppe chelate ring is not planar but exhibits an envelope conformation, i.e. the atoms Fe, P1, P2 and C(231) are essentially coplanar while atom C(131), the “flap” atom of the envelope, lies more than 0.73 Å away from this plane. The same applies to the other phosphane. The non-planarity of this conformation diminishes the contacts between the chelate phenyl groups and the nitrile ligand.

The compound displays a pseudo-fourfold rotation axis through H–Fe–N, relating the P atoms, which is almost perpendicular to the equatorial plane [87.6(5)°]. This equivalency of the P atoms agrees with the NMR spectroscopic data of the compounds, which show a quintuplet for the H ligand in their ^1H NMR spectra and a singlet for the four P atoms in their $^{31}\text{P}\{^1\text{H}\}$ NMR spectra. These results show that these molecules maintain in the solid state the general structure found in solution.

In the crystal packing, the molecules of compound **1** form pseudo-dimers with an antiparallel alignment due to a $C_{\text{ar}}\text{--}H\cdots O(1)_{\text{nitrile}}$ hydrogen-bond interaction [$D\text{--}A = 2.58(2)$ Å], thus cancelling their NLO responses in the crystalline state (Figure 2, a). Each constituent of this dimer is part of a chain in which the molecules are aligned due to the other $C_{\text{ar}}\text{--}H\cdots O(2)_{\text{nitrile}}$ hydrogen-bond interaction [$D\text{--}A = 2.58(2)$ Å] and also through the PF_6 anion, with $C\text{--}H\cdots F$ interactions [$C123\text{--}H\cdots F5 = 2.67(2)$, $C7\text{--}H\cdots F2 = 2.51(2)$, $C212\text{--}H\cdots F2 = 2.30(2)$, $C246\text{--}H\cdots F4 = 2.54(2)$, $C226\text{--}H\cdots F4 = 2.58(2)$, $C341\text{--}H\cdots F1 = 2.50(2)$ Å], which arrange the molecules in a straight line (along a). Overall, as can be seen in Figure 2 (b), the crystal structure is formed by alternating chains of molecules aligned in opposite directions. It can also be seen that, in each chain, the

Table 3. Structural data for pseudo-octahedral iron derivatives containing hydride and nitrile ligands.

Compound	Fe–H [Å]	Fe–N [Å]	N≡C [Å]	Reference
$[\text{Fe}(\text{H})(\text{dppe})_2(\text{NC}\text{--}\text{SCH}_3)][\text{CF}_3\text{SO}_3]$	1.45(3)	1.916(2)	1.153(3)	[23]
$[\text{Fe}(\text{H})(\text{dppe})_2(\text{NC}\text{--}\text{NH}_2)][\text{BF}_4]$	1.59(9)	1.95(1)	1.15(2)	[19]
$[\text{Fe}(\text{H})(\text{depe})_2(\text{NC}\text{--}\text{CHCOOEt})]$	1.50(6)	1.945(4)	1.167(6)	[24]
$[\text{Fe}(\text{H})(\text{dppe})_2(\text{NC}\text{--}\text{CH}_3)][\text{BPh}_4]$	1.50(2)	1.933(2)	1.141(3)	[18]
$[\text{Fe}(\text{H})(\text{dppe})_2(\text{NC}\text{--}\text{CH}_2\text{CH}_2\text{OMe})] [\text{BPh}_4]$	1.44(2)	1.930(2)	1.149(2)	[18]
$[\text{Fe}(\text{H})(\text{dppm})_2(\text{NC}\text{--}\text{CH}_3)] [\text{BF}_4]$	1.35(6)	1.927(4)	1.137(6)	[20]
$[\text{Fe}(\text{H})(\text{dppe})_2(\text{NC}\text{--}\text{C}_6\text{H}_4\text{NO}_2)] [\text{PF}_6]$ (1)	1.45(5)	1.880(5)	1.162(7)	this work

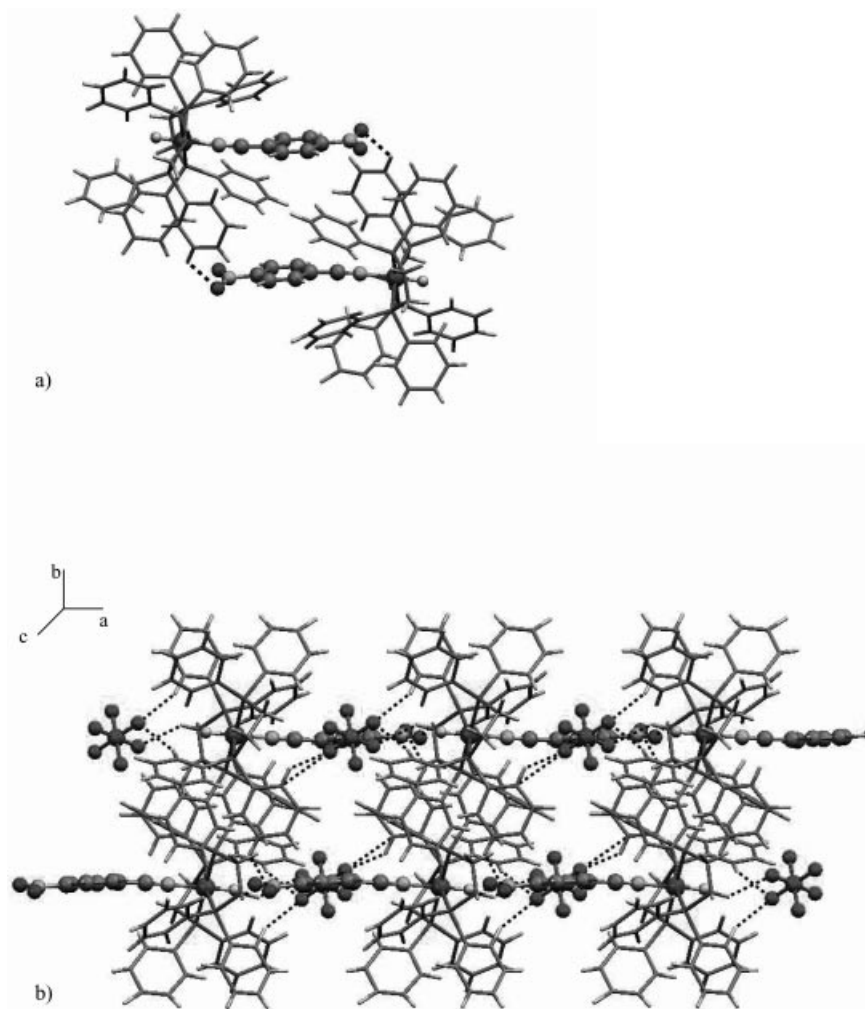


Figure 2. a) View of the antiparallel dimer; b) view of the crystal arrangement showing the alternating chains of cations aligned in opposite directions (solvent molecules have been omitted for clarity).

PF_6 anion occupies the “open space” to form an anion channel along *c*.

The second-order NLO response of compound **1** is cancelled in the solid state because of the pairwise antiparallel alignment of the chromophores, which results in a centrosymmetric structure. It has been shown previously that it is possible to overcome this problem of antiparallel alignment of neighbouring dipolar molecules by appropriate design of the molecular shape, in particular by introducing a spacer group between the successive chromophores.^[25,26] In this approach, the Coulomb interaction becomes equally favourable for the parallel alignment as for the antiparallel alignment of the chromophores. The actual crystal structure formed is then determined by more subtle factors, such as chirality, hydrogen bonding and steric (van der Waals) interactions. These considerations are the subject of a previous paper,^[25] where we have shown that this strategy works for complexes of very similar size and dipole moment. In fact, an ideal crystal structure with perfectly aligned chromophores was obtained for two cyclopentadienylruthenium and -iron complexes with chiral co-

ligands;^[25,27] in both cases the analogous complex with an achiral coligand crystallised centrosymmetrically. While the condition of proper spacing along the dipolar axis was met accurately in those Cp complexes,^[25] this spacing was hard to control. In view of these design strategies, the new complexes studied here, besides the obvious possibility to replace the dppe co-ligands with chiral phosphanes, have the additional advantage of an available valence *trans* to the nitrile ligand due to their pseudo-octahedral geometry. This should allow a better control of the spacing (adapted to the length of the dipolar chromophore) and thus enable optimisation of the microscopic and macroscopic NLO properties.

UV/Visible Studies

The electronic spectra of the compounds and of the uncoordinated nitrile ligands were recorded for 10^{-4} to 10^{-5} M chloroform solutions (Figure 3) in order to identify the M–L charge transfer and π – π^* absorption bands expected in

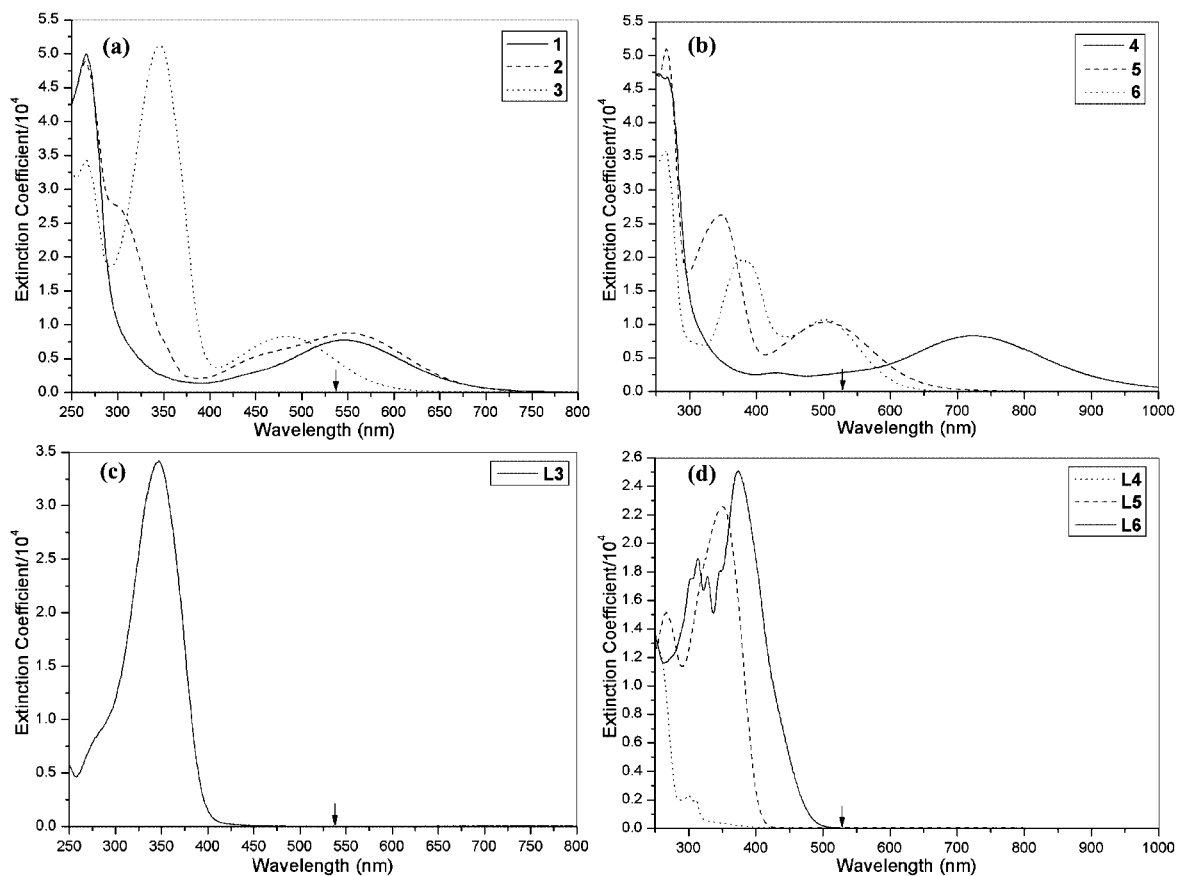


Figure 3. Optical absorption spectra of the compounds of Table 1: The nitro complexes (a) with an associated free ligand (c) and the dinitro complexes (b) with the free ligands (d). The downward arrow indicates the second harmonic wavelength of 536 nm at which most of the HRS measurements were performed.

these complexes. Additionally, a study of one of the compounds in other solvents was carried out to examine the solvatochromic effect.

The absorption bands in the 253–376 nm range are associated with the $\pi \rightarrow \pi^*$ and $n \rightarrow \pi^*$ transitions in the nitrile ligands, since they are also observed in this region for the corresponding free nitriles. Transitions at longer wavelengths (500–725 nm) are due to M–L charge transfer involving the Fe^{II} centre and the nitro-substituted aromatic nitrile and are explained by π back-donation involving $d_{\pi}(\text{Fe})-\pi^*(\text{NC})$ orbitals (see Table 1). Dinitro substitution of the aromatic nitrile, going from **1** to **4**, results in a red-shift of 177 nm for the MLCT band. Chain lengthening leads to different behaviours for the absorption bands in the spectra: while the short wavelength absorption band, associated with the $\pi-\pi^*$ transition of the conjugated nitrile ligand (250–375 nm range), displays a red-shift with increasing chain length, as would be expected, a reverse effect was observed for the lowest energy band. In fact, going from **1** to **3** (or from **4** to **5**) we can observe a blue-shift and a slight enhancement of the MLCT band. Such a blue-shift has been observed before for CT transitions in organic^[28,29] and organometallic^[30] strong push-pull systems, for which a lower energy charge-transfer transition is obtained when the donor and acceptor groups are well-coupled through a shorter conjugated path.

Sizable solvent-induced shifts of absorption maxima (solvatochromism) are a measure of the CT character of the transition (large change in dipole moment $\Delta\mu$), and therefore have been used as an indication of appreciable quadratic molecular hyperpolarisabilities β .^[27] It was therefore of interest to assess the solvatochromic response of the MLCT band for the complexes and $[\text{Fe}(\text{H})(\text{dppe})_2(4\text{-NCC}_6\text{H}_4\text{NO}_2)][\text{PF}_6]$ (**1**) was studied in solvents of different polarity (chloroform, acetone and DMSO). A positive solvatochromic shift of 21 nm across the range of these solvents was observed, with the lowest energy transition found in the polar solvent DMSO. This identifies this band as a CT transition and shows that the dipole moment increases upon excitation, consistent with a charge transfer from the metallic donor to the acceptor side of the complex.

Hyper-Rayleigh Scattering Measurements

The experimental resonant hyperpolarisabilities obtained by hyper-Rayleigh scattering (HRS) at 1072 nm for the series of compounds studied in this work and the chemical structures of the acceptor-substituted ligands are summarised in Table 1. In general, high β values are obtained for the complexes. HRS measurements were also performed on the free acceptor-substituted nitrile ligands, which exhibit

very low hyperpolarisabilities, in contrast to the corresponding push-pull systems.

To interpret the nearly resonant β values of the complexes in terms of electronic properties it is useful to consider the two-level model (TLM), which is based on the assumption that only one excited state [i.e. the charge transfer (CT) state] contributes to the β value. Assuming that the difference between the dipole moment in the ground and excited state, $\Delta\mu$, and the transition dipole, μ_{eg} , are parallel to each other (along the z -axis), the β tensor only has a diagonal zzz -component and can be written as^[3,31,32]

$$\beta_{zzz}(-2\omega; \omega, \omega) = \frac{3e^2 f_{osc} \Delta\mu}{2\hbar m \omega_{eg}^3} \cdot \frac{\omega_{eg}^4}{(\omega_{eg}^2 - \omega^2)(\omega_{eg}^2 - 4\omega^2)}$$

where f_{osc} is the oscillator strength of the CT transition and ω_{eg} its frequency. The expression consists of a static value, β_0 , multiplied by a wavelength-dependent resonance factor.

Because this model does not take into account the line broadening of the transition, it cannot be used to describe

the dispersion of β close to resonance. Hence, because most of the compounds studied in this work have a λ_{max} value close to the second harmonic wavelength of 536 nm, the model is not suitable to calculate static β values. To study the wavelength dependence of β in the NIR, and eventually derive a more reliable estimate of the static value β_0 , two of the compounds (**2** and **3**) were studied in the 1072–1580 nm range. These wavelength-dependent HRS data are presented in Figure 4, where a pronounced resonant enhancement associated with the low-energy charge-transfer transition can be seen in both cases.

The TLM curves based on the most resonant (1072 nm) and the least resonant β value (1540 nm, shown for **2** only) are also plotted in Figure 4. For compound **3**, which is not extremely resonant, the TLM curve going through the 1072 nm value appears to give quite a good description of the dispersion of β , and the obtained static value of 115×10^{-30} esu seems adequate. In fact, this curve is (coincidentally) overlapping with the one based on the 1580 nm

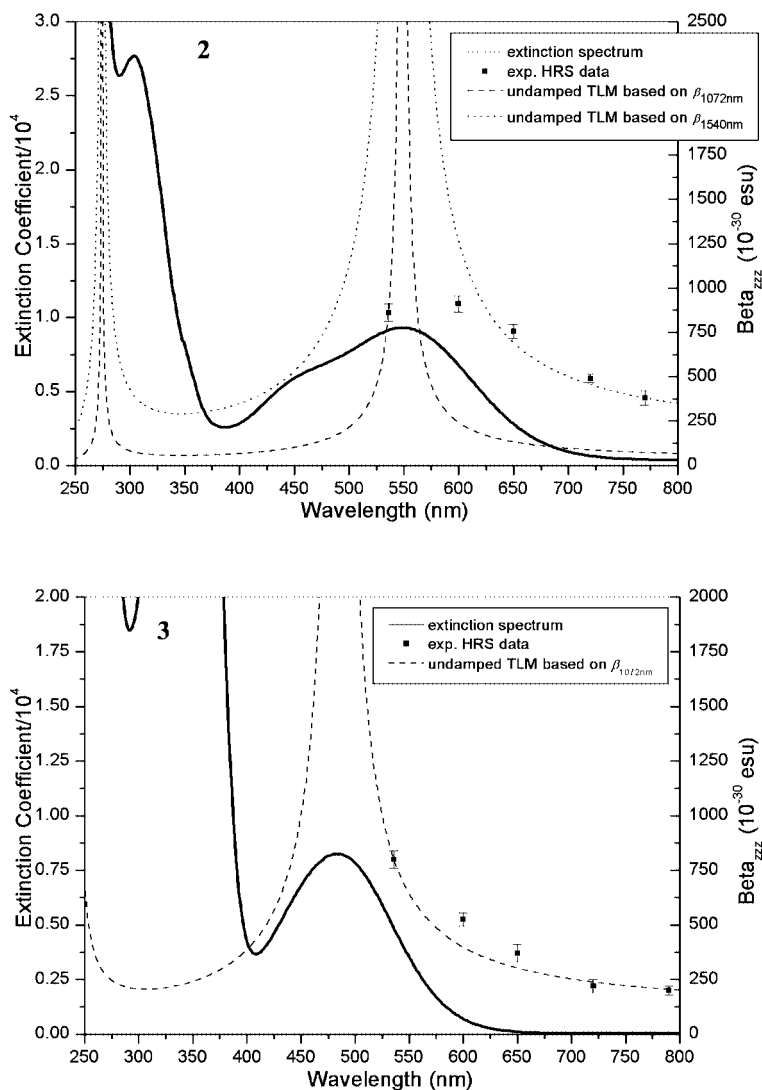


Figure 4. Wavelength-dependent HRS data for complexes **2** (top) and **3** (bottom) together with their extinction spectra. The two-level model (TLM) curves based on the most and least resonant β values are also shown (overlapping for **3**). For a clear view of the two-photon resonance, the experimental hyperpolarisabilities and the TLM curves are displayed at the frequency-doubled wavelength.

value, which leads to practically the same β_0 value (113×10^{-30} esu). Compound **2**, on the other hand, is closer to resonance and it is clearly seen that the undamped TLM is totally inadequate to derive the static value from β at 1072 nm. The dispersion is very poorly modelled and a far too low β_0 would be obtained using only this resonant value. However, using only the least resonant β (at 1540 nm) shows that the TLM gives a good description of the long wavelength tail of the dispersion curve and yields a more reliable static β_0 (163×10^{-30} esu). So, this wavelength-dependent HRS study clearly shows that the TLM cannot be used to calculate β_0 from strongly resonant hyperpolarisabilities and therefore, in the following discussion, we will use the TLM for only qualitative comparisons between the different structural variations. One way to improve on this model is to introduce an ad hoc damping factor, Γ , into the expression of β but, unfortunately, some additional complications arise in this procedure. Firstly, it is not clear whether such a damping factor (i.e. a homogeneous line-broadening) can also be used to properly describe the actual linewidth, which is largely due to inhomogeneous broadening and vibronic coupling, and secondly, there is a possible red-shift between the absorption and the β maximum, as reported by Wang et al.^[33] Therefore, more extended wavelength-dependent HRS measurements are needed to decide between different possible models.^[31,34–37]

The first structural variation which will be discussed is the replacement of the η^5 -monocyclopentadienyl ring at the organometallic donor fragment by a second bidentate phosphane (dppe) ligand to create a pseudo-octahedral surrounding of the iron moiety. Comparing **1** with **7** and **2** with **8** (see Table 1) we can see that in both cases the introduction of the second dppe ligand results in a red-shift of the CT band and an increase of the extinction coefficient, ϵ_{\max} , which results in an increase of the resonant β value, in agreement with the two-level model. From IR measurements a significant shift to lower $\nu(\text{N}\equiv\text{C})$ values was observed upon coordination ($\Delta\nu_{\text{NC}} = -56 \text{ cm}^{-1}$ for **1** and -43 cm^{-1} for **2**; see Table 1). This points to a stronger π back-donation and hence a higher donor efficiency in the pseudo-octahedral cases **1** and **2** as compared to the analogous cyclopentadienyl compounds **7** and **8**, where a shift of only -35 and -15 cm^{-1} was found, respectively.^[12] This is indeed supported by the higher static value of 163×10^{-30} esu obtained for the pseudo-octahedral compound **2** than the β_0 of 112×10^{-30} esu for the analogous cyclopentadienyl complex **8**.^[12] So, in conclusion, based on the spectroscopic measurements and the increase of the static β value it appears that the pseudo-octahedral surrounding yields a more efficient electron donor.

A second strategy we used to optimise the push-pull system was to also increase the strength of the electron-withdrawing moiety by introducing an extra nitro group at the *ortho* position of the last phenyl ring of the conjugated backbone. Comparing compounds **1** and **4** and **3** and **5** we can see that in both cases the introduction of the second nitro group results in a shift of the CT band to higher wavelengths and an increase of the extinction coefficient. It ap-

pears that introducing the second nitro group results in a more efficient electron-withdrawing moiety, thereby lowering the energy of the CT transition. The energy shift makes the longer compound **5** more resonant than compound **3**, while for the shorter compound **4**, the shift is much more drastic and results in a CT band in the NIR, beyond resonance. However, compound **4** has a remarkably high β value, taking into account that it is farther from resonance, so it probably has a higher static value β_0 than compound **1**.

The smaller red-shift observed for the longer compounds (**3** and **5**) can be understood by considering that the second nitro group was introduced on the second phenyl ring, farther from the donor metal fragment, leading to a less effective D–A interaction through the π back-donation effect.

The third degree of freedom which can be used to optimise the molecular β value is the structure and length of the conjugated backbone connecting the electron donor and acceptor. It is well known that β increases sharply with conjugation length, therefore we extended the conjugated backbone of both the nitro (**1**, **2** and **3**) and the dinitro compounds (**4** and **5**). A very surprising result is that, for both forms, the CT band shifts to higher energy for the longer compounds. As we mentioned previously, this can be explained by a better interaction of the donor with the acceptor through the shorter conjugated path, leading to a very low energy CT transition. However, the longer compound **2** yields a larger β than the shorter one **1**, which in this case is compatible with the difference in extinction coefficients, ϵ_{\max} . This trend is continued for the even longer compound **3**. Indeed, comparing compounds **2** and **3** we see that although compound **3** is much less resonant and has about the same extinction coefficient, it still has a comparable β value to compound **2**. This points to a large static β value for compound **3** as a consequence of a large dipole moment difference, according to the two-level model. In the case of the dinitro compounds the difference between the β values of the shorter compound **4** and the longer one **5** can be explained in terms of resonant enhancement and difference between extinction coefficients.

Finally, the structural change of introducing one hydrazone spacer ($-\text{C}=\text{N}-\text{NH}$) between the two phenyl rings forming the backbone on going from compound **5** to **6** seems to have virtually no effect on the β values; $\nu(\text{N}\equiv\text{C})$, $\delta_{\text{H}_{\text{hydride}}}$ and $\delta_{\text{N}_{\text{dppe}}}$ (see Table 1) also remain unchanged, and only $\nu(\text{Fe}-\text{H})$ is slightly higher. Neither the spectral position of the CT band nor the extinction coefficient is modified significantly so it seems that the D–A interaction is barely changed by this last modification.

In conclusion, a series of hydrido(nitrile)iron(II) complexes have been synthesised that show improved molecular NLO properties, which we ascribe to an improved donor character of the pseudo-octahedral organometallic moiety. The NLO push-pull system was further improved by increasing the conjugation length and by double nitro substitution to form a better electron-accepting moiety. Wavelength-dependent HRS measurements, performed for the first time on organometallic NLO chromophores, show the

effect of two-photon resonance enhancement and demonstrate that for highly resonant cases the TLM is inadequate and therefore wavelength-dependent measurements are needed to model the dispersion of β . The X-ray structure of $[\text{Fe}(\text{H})(\text{dppe})_2(4\text{-NCC}_6\text{H}_4\text{NO}_2)][\text{PF}_6^-]$ (**1**) showed that the NLO response is cancelled at the macroscopic level for this compound by a pairwise antiparallel orientation of the complexes. However, the pseudo-octahedral coordination appears to be very suitable for a more systematic implementation of the previously demonstrated^[25,27] design strategies (replacement of dppe by chiral phosphanes and inclusion of appropriate spacing groups along the dipolar axis) to promote a favourable non-centrosymmetric crystal structure.

Experimental Section

General Procedures: All preparations were carried out under vacuum or nitrogen using standard Schlenk techniques. The solvents were dried before use following published methods.^[38] The starting material $[\text{FeHCl}(\text{dppe})_2]$ was synthesised according to a published method.^[39] The aromatic nitrile ligands 4-nitrobenzotrile and 2,4-dinitrobenzotrile were purchased from Sigma–Aldrich and used as received. Ligands (*E*)-4-[2-(4-nitrophenyl)ethenyl]benzotrile,^[40] (*E*)-3-(4-nitrophenyl)acrylonitrile,^[41] 4-[*N*-(2,4-dinitrophenyl)hydrazonomethyl]benzotrile^[42] and (*E*)-4-[2-(2,4-dinitrophenyl)ethenyl]benzotrile^[43] were prepared following the literature procedures.

IR spectra were recorded for KBr pellets on a Perkin–Elmer Paragon 1000 PC FT-IR or a Bio-Rad Excalibur FTS 3000MX spectrophotometer; only the significant bands are cited. ^1H , ^{13}C and ^{31}P NMR spectra were recorded for $[\text{D}_2]$ dichloromethane solutions with a Varian Unity 300 spectrometer at probe temperature, using SiMe_4 as internal reference (^1H and ^{13}C NMR chemical shifts) and 85% H_3PO_4 as external reference for ^{31}P NMR chemical shifts. Spectral assignments follow the numbering scheme given in Scheme 1. The UV/Vis spectra were recorded with a Shimadzu 1603 spectrophotometer for 10^{-4} or 10^{-5} M solutions in several solvents. Elemental analyses were performed at the Laboratório de Análises de the Instituto Superior Técnico, using a Fisons Instruments EA1108 system, with data acquisition, integration and handling performed with a PC and the software package Eager-200 (Carlo Erba Instruments). Melting points were measured with a Leica Galen III melting point apparatus and are not corrected.

General Procedure for the Synthesis of the Pseudo-Octahedral Iron(II) Derivatives: A slight excess of the nitrile chromophore (1.1–1.2 equiv.) and TlPF_6 (1.1–1.2 equiv.) were added to a solution of $[\text{Fe}(\text{H})(\text{Cl})(\text{dppe})_2]$ (0.68–1.01 mmol) in dichloromethane (THF for compound **1**). The mixture was then stirred at room temperature for 2–4 h (18 h for compounds **1** and **6**). A colour change was observed with simultaneous precipitation of thallium chloride. After filtration, the solvents were evaporated under vacuum to dryness and the residues were washed several times with diethyl ether to remove the excess of nitrile. Recrystallisation from dichloromethane/diethyl ether afforded powder or crystalline samples of the pure compounds.

$[\text{Fe}(\text{H})(\text{dppe})_2(4\text{-NCC}_6\text{H}_4\text{NO}_2)][\text{PF}_6^-]$ (1**):** Yield: 97 mg (37%), purple crystals; m.p. 132.7–134.2 °C. IR (KBr): $\tilde{\nu}_{\text{max}} = 2177 \text{ cm}^{-1}$ (s) (CN), 1870 (w) (Fe–H), 1516 (m) and 1338 (s) (NO_2), 838 (s) (PF_6^-). ^1H NMR (300 MHz, CD_2Cl_2): $\delta = -17.48$ (quint, $^2J_{\text{H,P}} =$

47.6 Hz, 1 H, FeH), 2.13 (s, 4 H, PCH_2), 2.59 (s, 4 H, PCH_2), 6.73 (d, $J = 8.4$ Hz, 2 H, H2,H6), 6.77 (s, 8 H, PPh-H_{ortho}), 7.07 (t, $J = 7.5$ Hz, 8 H, PPh-H_{meta}), 7.18 (t, $J = 7.5$ Hz, 8 H, PPh-H_{meta}), 7.27–7.36 (m, 8 H, PPh-H_{para}), 7.47 (s, 8 H, PPh-H_{ortho}), 8.18 (d, $J = 8.4$ Hz, 2 H, H3,H5) ppm. $^{13}\text{C}\{^1\text{H}\}$ NMR (CD_2Cl_2): $\delta = 32.54$ (qt, $^1J_{\text{C,P}} = 11.4$ Hz, PCH_2), 118.81 (C1), 123.11 (NC), 124.56 (C3,C5), 128.35 and 129.11 (PPh-C_{meta}), 130.46 and 130.60 (PPh-C_{para}), 132.70 (PPh-C_{ortho}), 132.97 (C2,C6), 133.38 (PPh-C_{ortho}), 134.64 (m, PPh-C_{ipso}), 149.24 (C4) ppm. $^{31}\text{P}\{^1\text{H}\}$ NMR (CD_2Cl_2): $\delta = -143.50$ (sept, $^1J_{\text{P,F}} = 709.2$ Hz, PF_6), 83.34 (s, dppe) ppm. $\text{C}_{59}\text{H}_{53}\text{F}_6\text{FeN}_2\text{O}_2\text{P}_5 \cdot 1/2\text{CH}_2\text{Cl}_2$ (1190.3) calcd. C 60.09, H 4.58, N 2.36; found C 60.31, H 4.64, N 2.27. UV (CHCl_3): $\lambda_{\text{max}}(\epsilon) = 265 \text{ nm}$ ($49937 \text{ M}^{-1}\text{cm}^{-1}$), 546 (7706); $[(\text{CH}_3)_2\text{CO}]$: 535 (8155); (DMSO): 266 (73979), 556 (11263).

$[\text{Fe}(\text{H})(\text{dppe})_2\{(E)\text{-4-NCC}_6\text{H}_4\text{CH}=\text{CHC}_6\text{H}_4\text{NO}_2\}][\text{PF}_6^-]$ (2**):** Yield, 380 mg (48%), purple solid; m.p. 134.2–135.7 °C. IR (KBr): $\tilde{\nu}_{\text{max}} = 2174 \text{ cm}^{-1}$ (s) (CN), 1853 (w) (Fe–H), 1515 (m) and 1339 (s) (NO_2), 839 (s) (PF_6^-). ^1H NMR (300 MHz, CD_2Cl_2): $\delta = -18.03$ (quint, $^2J_{\text{H,P}} = 46.8$ Hz, 1 H, FeH), 2.12 (s, 4 H, PCH_2), 2.61 (s, 4 H, PCH_2), 5.65 (d, $J = 15.9$ Hz, 1 H, H8), 6.22 (d, $J = 15.9$ Hz, 1 H, H7), 6.76 (s, 8 H, PPh-H_{ortho}), 7.17 (t, $J = 6.6$ Hz, 16 H, PPh-H_{meta}), 7.26–7.37 (m, 8 H, PPh-H_{para}), 7.49 (s, 10 H, PPh-H_{ortho} and H2,H6), 8.26 (d, $J = 7.5$ Hz, 2 H, H3,H5) ppm. $^{13}\text{C}\{^1\text{H}\}$ NMR (CD_2Cl_2): $\delta = 32.80$ (t, $^1J_{\text{C,P}} = 12.0$ Hz, PCH_2), 101.10 (C8), 124.58 (NC), 124.69 (C3,C5), 128.12 (C2,C6), 128.23 and 128.90 (PPh-C_{meta}), 130.22 and 130.45 (PPh-C_{para}), 132.79 and 133.43 (PPh-C_{ortho}), 134.07 and 135.07 (m, PPh-C_{ipso}), 139.83 (C1), 146.73 (C7), 148.16 (C4) ppm. $^{31}\text{P}\{^1\text{H}\}$ NMR (CD_2Cl_2): $\delta = -143.50$ (quint, $^1J_{\text{P,F}} = 710.1$ Hz, PF_6), 83.80 (s, dppe) ppm. $\text{C}_{61}\text{H}_{55}\text{F}_6\text{FeN}_2\text{O}_2\text{P}_5$ (1172.8) calcd. C 62.47, H 4.73, N 2.39; found C 62.88, H 4.70, N 2.73. UV (CHCl_3): $\lambda_{\text{max}}(\epsilon) = 265 \text{ nm}$ ($48916 \text{ M}^{-1}\text{cm}^{-1}$), 297 (27695), 549 (8762).

$[\text{Fe}(\text{H})(\text{dppe})_2\{(E)\text{-4-NCC}_6\text{H}_4\text{CH}=\text{CH-4-C}_6\text{H}_4\text{NO}_2\}][\text{PF}_6^-]$ (3**):** Yield: 900 mg (71%), dark-red solid; m.p. 145.1–145.9 °C. IR (KBr): $\tilde{\nu}_{\text{max}} = 2185 \text{ cm}^{-1}$ (w) (NC), 1888 (w) (Fe–H), 1510 (m) and 1339 (s) (NO_2), 830 (s) (PF_6^-). ^1H NMR (300 MHz, CD_2Cl_2): $\delta = -18.83$ (quint, $^2J_{\text{H,P}} = 47.0$ Hz, 1 H, FeH), 2.12 (s, 4 H, PCH_2), 2.55 (s, 4 H, P-CH_2), 6.76 (d, $J = 8.1$ Hz, 2 H, H2,H6), 6.85 (s, 8 H, PPh-C_{ortho}), 7.09 (t, $J = 7.5$ Hz, 8 H, PPh-C_{meta}), 7.16 (t, $J = 7.5$ Hz, 8 H, PPh-C_{meta}), 7.25–7.36 (m, 10 H, PPh-C_{para}), H7 and H8), 7.45 (s, 8 H, PPh-C_{ortho}), 7.57 (d, $J = 8.4$ Hz, 2 H, H3,H5), 7.74 (d, $J = 9.0$ Hz, 2 H, H10,H14), 8.27 (d, $J = 9.0$ Hz, 2 H, H11,H13) ppm; some signals are obscured by the *para* aromatic protons of dppe. $^{13}\text{C}\{^1\text{H}\}$ NMR (CD_2Cl_2): $\delta = 32.47$ (t, $J = 12.2$ Hz, PCH_2), 111.95 (C1), 124.24 (C11,C13), 126.43 (NC), 127.66 (C10,C14), 127.91 (C3,C5), 128.05 and 128.85 (PPh-C_{meta}), 129.98 (C7), 130.12 (PPh-C_{para}), 131.35 (C8), 132.34 (C2,C6), 132.65 and 133.20 (PPh-C_{ortho}), 133.97 and 134.95 (m, PPh-C_{ipso}), 140.79 (C4), 142.97 (C9), 147.45 (C12) ppm. $^{31}\text{P}\{^1\text{H}\}$ NMR (CD_2Cl_2): $\delta = -143.47$ (sept, $^1J_{\text{P,F}} = 708.6$ Hz, PF_6), 84.71 (s, dppe) ppm. $\text{C}_{67}\text{H}_{59}\text{F}_6\text{FeN}_2\text{O}_2\text{P}_5 \cdot \text{CH}_2\text{Cl}_2$ (1257.7) calcd. C 60.78, H 4.64, N 2.31; found C 60.71, H 4.96, N 1.99. UV (CHCl_3): $\lambda_{\text{max}}(\epsilon) = 266 \text{ nm}$ ($34316 \text{ M}^{-1}\text{cm}^{-1}$), 346 (51278), 485 (8255).

$[\text{Fe}(\text{H})(\text{dppe})_2\{2,4\text{-NCC}_6\text{H}_3(\text{NO}_2)_2\}][\text{PF}_6^-]$ (4**):** Yield: 386 mg (48%), dark-green solid; m.p. 144.4 °C (dec.). IR (KBr): $\tilde{\nu}_{\text{max}} = 2138 \text{ cm}^{-1}$ (m) (NC), 1891 (w) (Fe–H), 1527 (m) and 1338 (d) (NO_2), 839 (s) (PF_6^-). ^1H NMR (300 MHz, CD_2Cl_2): $\delta = -14.60$ (quint, $^2J_{\text{H,P}} = 48.5$ Hz, 1 H, FeH), 2.31 (s, 4 H, PCH_2), 2.88 (s, 4 H, PCH_2), 5.43 (d, $J_{\text{H}_6,\text{H}_5} = 9.0$ Hz, 1 H, H6), 6.72 (s, 8 H, PPh-C_{ortho}), 6.99 (t, $J = 7.5$ Hz, 8 H, PPh-C_{meta}), 7.16–7.25 (m, 12 H, PPh-C_{meta} and PPh-C_{para}), 7.30 (t, $J = 6.9$ Hz, 4 H, PPh-C_{para}), 7.43 (s, 8 H, PPh-C_{ortho}), 7.90 (dd, $J_{\text{H}_5,\text{H}_6} = 8.4$, $^4J_{\text{H}_5,\text{H}_3} = 2.4$ Hz, 1 H, H5), 8.99 (d, $^4J_{\text{H}_3,\text{H}_5}$

= 2.4 Hz, 1 H, H3) ppm. $^{13}\text{C}\{^1\text{H}\}$ NMR (CD_2Cl_2): δ = 32.95 (s, PCH_2), 113.97 (C1), 118.70 (NC), 121.66 (C3), 127.50 (C5), 128.40 and 129.16 (PPh-*Cmeta*), 130.66 and 130.85 (PPh-*Cpara*), 132.76 and 133.44 (PPh-*Cortho*), 134.38 (m, PPh-*Cipso*), 138.07 (C6), 146.78 and 147.24 (C2 and C4) ppm. $^{31}\text{P}\{^1\text{H}\}$ NMR (300 MHz, CD_2Cl_2): δ = -143.50 (sept, $^1J_{\text{P,F}} = 708.9$ Hz, PF_6), 81.00 (s, dppe) ppm. $\text{C}_{59}\text{H}_{52}\text{F}_6\text{FeN}_3\text{O}_4\text{P}_5 \cdot 1/2\text{CH}_2\text{Cl}_2$ (1237.7) calcd. C 57.90, H 4.33, N 3.40; found C 57.46, H 4.47, N 3.36. UV (CHCl_3): λ_{max} (ϵ) = 254 nm (shoulder), 266 (shoulder), 723 ($8274 \text{ M}^{-1} \text{ cm}^{-1}$).

[Fe(H)(dppe) $_2$ {(E)-4-NCC $_6$ H $_4$ CH=CH-2,4-C $_6$ H $_3$ (NO $_2$) $_2$ }][PF $_6$] (5): Yield: 444 mg (51%), purple solid; m.p. 161.9–163.6 °C. IR (KBr): $\tilde{\nu}_{\text{max}} = 2182 \text{ cm}^{-1}$ (w) (NC), 1891 (w) (Fe–H), 1528 (m) and 1345 (m) (NO $_2$), 840 (s) (PF_6^-). ^1H NMR (300 MHz, CD_2Cl_2): δ = -18.67 (quint, $^2J_{\text{H,P}} = 47.4$ Hz, 1 H, FeH), 2.11 (s, 4 H, PCH_2), 2.55 (s, 4 H, PCH_2), 6.77 (d, $J = 7.8$ Hz, 2 H, H2,H6), 6.83 (s, 8 H, PPh-*Cortho*), 7.09 (t, $J = 7.5$ Hz, 8 H, PPh-*Cmeta*), 7.16 (t, $J = 7.2$ Hz, 8 H, PPh-*Cmeta*), 7.28 (t, $J = 7.5$ Hz, 4 H, PPh-*Cpara*), 7.35 (t, $J = 7.2$ Hz, 4 H, PPh-*Cpara*), 7.46 (s, 8 H, PPh-*Cortho*), 7.60 (d, $J = 7.5$ Hz, 2 H, H3,H5), 7.73 (d, $J = 15.3$ Hz, 1 H, H8), 8.08 (d, $J = 8.7$ Hz, 1 H, H14), 8.52 (dd, $J_{\text{H13,H14}} = 8.7$, $^4J_{\text{H13,H11}} = 1.8$ Hz, 1 H, H13), 8.86 (d, $J_{\text{H11,H13}} = 2.4$ Hz, 1 H, H11) ppm; the signal for H7 is obscured by the *para* aromatic protons of dppe. $^{13}\text{C}\{^1\text{H}\}$ NMR (CD_2Cl_2): δ = 32.60 (t, $^1J_{\text{C,P}} = 11.7$ Hz, PCH_2), 113.07 (C1), 120.97 (C11), 125.42 (C8), 126.28 (NC), 127.98 (C13), 128.28 (PPh-*Cmeta*), 128.33 (C3,C5), 129.01 (PPh-*Cmeta*), 130.24 (C14), 130.37 and 130.44 (PPh-*Cpara*), 132.44 (C2,C6), 132.83 and 133.42 (PPh-*Cortho*), 134.14 and 135.14 (2 m, PPh-*Cipso*), 135.76 (C7), 138.24 (C4), 140.05 (C9), 147.29 and 148.04 (C10 and C12) ppm. $^{31}\text{P}\{^1\text{H}\}$ NMR (CD_2Cl_2): δ = -143.73 (quint, $^1J_{\text{P,F}} = 708.0$ Hz, PF_6), 83.48 (s, dppe) ppm. $\text{C}_{67}\text{H}_{58}\text{F}_6\text{FeN}_3\text{O}_4\text{P}_5$ (1293.9) calcd. C 62.19, H 4.52, N 3.25; found C 61.98, H 4.33, N 3.23. UV (CHCl_3): λ_{max} (ϵ) = 265 nm ($50967 \text{ M}^{-1} \text{ cm}^{-1}$), 349 (26449), 505 (10348).

[Fe(H)(dppe) $_2$ {4-NCC $_6$ H $_4$ CH=N-NH-2,4-C $_6$ H $_3$ (NO $_2$) $_2$ }][PF $_6$] (6): Yield: 440 mg (50%), dark-red solid; m.p. 153.5–155.4 °C. IR (KBr): $\tilde{\nu}_{\text{max}} = 3289 \text{ cm}^{-1}$ (w) (N–H), 2183 (w) (NC), 1896 (w) (Fe–H), 1616 (m) (C=N), 1513 (m) and 1333 (m) (NO $_2$), 841 (s) (PF_6^-). ^1H NMR (300 MHz, CD_2Cl_2): δ = -18.54 (quint, $^2J_{\text{H,P}} = 47.6$ Hz, 1 H, FeH), 2.12 (s, 4 H, PCH_2), 2.56 (s, 4 H, PCH_2), 6.79 (d, $J = 9.3$ Hz, 2 H, H2,H6), 6.83 (s, 8 H, PPh-*Cortho*), 7.10 (t, $J = 7.8$ Hz, 8 H, PPh-*Cmeta*), 7.17 (t, $J = 7.5$ Hz, 8 H, PPh-*Cmeta*), 7.28 (t, $J = 7.5$ Hz, 4 H, PPh-*Cpara*), 7.35 (t, $J = 7.2$ Hz, 4 H, PPh-*Cpara*), 7.46 (s, 8 H, PPh-*Cortho*), 7.79 (d, $J = 8.4$ Hz, 2 H, H3,H5), 8.17 (d, $J = 8.7$ Hz, 1 H, H13), 8.20 (s, 1 H, H7), 8.44 (dd, $J_{\text{H12,H13}} = 9.6$, $^4J_{\text{H12,H10}} = 2.4$ Hz, 1 H, H12), 9.15 (d, $J_{\text{H10,H12}} = 2.7$ Hz, 1 H, H10), 11.44 (s, 1 H, NH) ppm. $^{13}\text{C}\{^1\text{H}\}$ NMR (CD_2Cl_2): δ = 32.64 (t, $^1J_{\text{C,P}} = 12.20$ Hz, PCH_2), 114.08 (C1), 117.31 (C10), 123.65 (C12), 126.03 (NC), 128.18 (C3,C5), 128.31 and 129.05 (PPh-*Cmeta*), 130.40 and 130.48 (PPh-*Cpara*), 132.41 (C2,C6), 132.84 and 133.43 (PPh-*Cortho*), 134.14 and 135.12 (2 m, PPh-*Cipso*), 137.15 (C12), 137.55 (C4), 138.02 (C7), 139.32 (C8), 144.93 and 145.74 (C9 and C11) ppm. $^{31}\text{P}\{^1\text{H}\}$ NMR (CD_2Cl_2): δ = -143.66 (quint, $^1J_{\text{P,F}} = 707.2$ Hz, PF_6), 83.45 (s, dppe) ppm. $\text{C}_{66}\text{H}_{58}\text{F}_6\text{FeN}_5\text{O}_4\text{P}_5 \cdot \text{C}_4\text{H}_{10}\text{O}$ (1309.90) calcd. C 58.77, H 4.93, N 5.35; found C 58.91, H 4.59, N 4.90. UV (CHCl_3): λ_{max} (ϵ) = 266 nm ($35898 \text{ M}^{-1} \text{ cm}^{-1}$), 380 (19559), 503 (10679).

Crystal Structure of 1: $\text{C}_{59}\text{H}_{53}\text{F}_6\text{FeN}_2\text{O}_2\text{P}_5 \cdot \text{CH}_2\text{Cl}_2$, $M = 1231.66$, $\mu = 4.774 \text{ mm}^{-1}$, $\rho = 1410 \text{ mg m}^{-3}$, monoclinic, $P2_1/n$, $Z = 4$, $a = 12.48(1)$, $b = 35.599(9)$, $c = 13.243(9) \text{ \AA}$, $\beta = 99.49(2)^\circ$, $V = 5803(6) \text{ \AA}^3$, from 23 reflections ($16.7^\circ < 2\theta < 18.9^\circ$). Cell dimensions and intensities were measured at 293(2) K with an Enraf–Nonius TURBOCAD4 diffractometer (Cu rotating anode, $\lambda = 1.54180 \text{ \AA}$). As a general procedure, the intensity of three standard

reflections was measured periodically every 5 h. This procedure did not reveal any appreciable decay. Using the CAD4 software, data were corrected for Lorentz and polarisation effects and empirically for absorption (from Ψ -scan measurements). Data were collected in the range $3.6^\circ < \theta < 67^\circ$ ($-13 < h < 14$, $0 < k < 42$, $0 < l < 15$); 10579 measured reflections, 10140 of which were considered as observed [$|F_o|^2 > 3\sigma(|F_o|^2)$]; $R_{\text{int}} = 0.0503$ for equivalent reflections. The structure was solved by direct methods using SIR97^[44] and refined with SHELXL^[45] in the WINGX^[46] program package. Full-matrix least-squares refinement based on F^2 gave final values $R = 0.0729$, $wR_2 = 0.1397$ for 923 variables and 10140 contributing reflections. The position of the Fe atom was obtained from a three-dimensional Patterson synthesis, while all the other non-hydrogen atoms were located in subsequent difference Fourier maps. The hydrogen atoms were inserted in calculated positions and refined isotropically as riding on the parent carbon atom. The final difference electron density map showed a maximum of 0.558 and a minimum of $-0.695 \text{ e \AA}^{-3}$.

CCDC-286415 contains the supplementary crystallographic data for this paper. These data can be obtained free of charge from The Cambridge Crystallographic Data Centre via www.ccdc.cam.ac.uk/data_request/cif.

Hyper-Rayleigh Scattering Measurements: First hyperpolarisabilities were determined by means of the hyper-Rayleigh scattering (HRS) technique.^[47,48] The measurements were performed in a new HRS setup based on an optical parametrical amplifier (OPA) pumped by a Ti:sapphire regenerative amplifier (pulse width: 2 ps, repetition rate: 1.5 kHz, average power: ca. 30 mW). The different fundamental wavelengths used (1072, 1200, 1300, 1440, 1540 and 1580 nm) were obtained by tuning the signal beam of the OPA, and were chosen carefully to avoid vibrational absorption bands of chloroform. To prevent dielectric breakdown and self-focusing, the pulses were focused onto the sample with cylindrical lenses. The scattered second harmonic light was collected at 90° and detected with a combination of a spectrograph and an intensified charge coupled device (ICCD) with red-sensitive photocathode. The ICCD provides nanosecond-gated parallel detection of a small (ca. 23 nm) spectral area around the harmonic wavelength. The outer regions of this range was used to correct the HRS signal for multi-photon fluorescence, as described before.^[4,10] A large photoluminescence background was only observed for one of the free ligands (L3, see Table 1), for which the luminescence signal, integrated over the central region of 6 nm, was about equal to the actual HRS signal. HRS measurements were performed in a rectangular fused silica cell containing a dilute solution of the compound in chloroform. Concentrations used were of the order of 10^{-6} – 10^{-4} M for the complexes and 10^{-3} – 10^{-4} M for the free ligands. With these concentrations the absorption of the second harmonic wavelength was kept well below 10%, so that an accurate correction for this effect could be carried out. The absorption measurements were performed with a Varian Cary 5 absorption spectrometer. All hyperpolarisabilities were determined by internal reference relative to chloroform,^[48] as described before.^[4,10] Within the assumption of only one significant diagonal β tensor component along the z -axis (i.e. the conjugated backbone of the molecule), β_{zzz} values can be calculated by measuring the HRS signal for a dilute solution with known concentration of the chromophores and from pure chloroform. The β value of 0.49×10^{-30} esu for chloroform, determined with the EFISHG technique at 1064 nm,^[49] was used as internal reference. The dispersion of the reference value in the explored 1072–1580 nm range was neglected. An upper limit of 5% to this effect was estimated using the TLM expression with the maximum of the longest wavelength absorption band of chloroform (143 nm)^[50] taken as λ_{eg} .

Acknowledgments

Financial support for this work was provided by the TMR network programme "Organometallic dipoles with NLO properties" contract ERBFMRXCT-CT98-0166, by COST D14, and partly by the Fundação para a Ciência e Tecnologia and POCTI (POCTI/QUI/48443/2002). W.W. is a Postdoctoral Fellow of the Fund for Scientific Research of Flanders (Belgium) (FWO, Vlaanderen). Financial support from the FWO in the group project G.0041.01 is gratefully acknowledged.

- [1] M. L. H. Green, S. R. Marder, M. E. Thompson, J. A. Bandy, D. Bloor, P. V. Kolinsky, R. J. Jones, *Nature* **1987**, *330*, 360–362.
- [2] H. S. Nalwa, *Appl. Organomet. Chem.* **1991**, *5*, 349–377 and references cited therein.
- [3] P. N. Prasad, D. J. Williams, *Introduction to Nonlinear Optical Effects in Molecules and Polymers*, John Wiley and Sons, Inc., New York, **1991**.
- [4] E. Goovaerts, W. Wenseleers, M. H. Garcia, G. H. Cross, *Handbook of Advanced Electronic and Photonic Materials and Devices* (Ed.: H. S. Nalwa), Academic Press, **2001**, vol. 9, p. 127–191 and references cited therein.
- [5] I. R. Whittall, A. M. McDonagh, M. G. Humphrey, M. Samoc, *Adv. Organomet. Chem.* **1999**, *43*, 349–405 and references cited therein.
- [6] S. Di Bella, *Chem. Soc. Rev.* **2001**, *30*, 355–366 and references cited therein.
- [7] C. E. Powell, M. G. Humphrey, *Coord. Chem. Rev.* **2004**, *248*, 725–756 and references cited therein.
- [8] J. Zyss, *Molecular Nonlinear Optics: Materials, Physics, and Devices*, Academic Press, San Diego, CA, **1994**.
- [9] J. C. Calabrese, L. T. Cheng, J. C. Green, S. R. Marder, W. Tam, *J. Am. Chem. Soc.* **1991**, *113*, 7227–7232.
- [10] W. Wenseleers, A. W. Gerbrandij, E. Goovaerts, M. H. Garcia, M. P. Robalo, P. J. Mendes, J. C. Rodrigues, A. R. Dias, *J. Mater. Chem.* **1998**, *8*, 925–930.
- [11] M. H. Garcia, M. P. Robalo, A. R. Dias, M. T. Duarte, W. Wenseleers, G. Aerts, E. Goovaerts, M. P. Cifuentes, S. Hurst, M. G. Humphrey, M. Samoc, B. Luther-Davies, *Organometallics* **2002**, *21*, 2107–2118.
- [12] M. H. Garcia, M. P. Robalo, A. R. Dias, M. F. M. Piedade, A. Galvão, W. Wenseleers, E. Goovaerts, *J. Organomet. Chem.* **2001**, *619*, 252–264.
- [13] A. M. McDonagh, M. G. Humphrey, M. Samoc, B. Luther-Davies, *Organometallics* **1999**, *18*, 5195–5197.
- [14] H. Le Bozec, T. Le Bouder, O. Maury, A. Bondon, I. Ledoux, S. Deveau, J. Zyss, *Adv. Mater.* **2001**, *13*, 1677–1681.
- [15] A. M. McDonagh, I. R. Whittall, M. G. Humphrey, B. W. Skelton, A. H. White, *J. Organomet. Chem.* **1996**, *519*, 229–235.
- [16] R. H. Naulty, A. M. McDonagh, I. R. Whittall, M. P. Cifuentes, M. G. Humphrey, S. Houbrechts, J. Maes, A. Persoons, G. A. Heath, D. C. R. Hockless, *J. Organomet. Chem.* **1998**, *563*, 137–146.
- [17] I. R. Whittall, M. P. Cifuentes, M. G. Humphrey, B. Luther-Davies, M. Samoc, S. Houbrechts, A. Persoons, G. A. Heath, D. C. R. Hockless, *J. Organomet. Chem.* **1997**, *549*, 127–137.
- [18] J. G. Lee, B. S. Yoo, N. S. Choi, K. I. Park, S. I. Cho, C. M. Lee, S. W. Lee, *J. Organomet. Chem.* **1999**, *589*, 138–149.
- [19] L. Martins, J. da Silva, A. J. L. Pombeiro, R. A. Henderson, D. J. Evans, F. Benetollo, G. Bombieri, R. A. Michelin, *Inorg. Chim. Acta* **1999**, *291*, 39–48.
- [20] Y. Gao, D. G. Holah, A. N. Hughes, G. J. Spivak, M. D. Havighurst, V. R. Magnuson, *Polyhedron* **1998**, *17*, 3881–3888.
- [21] M. H. Garcia, M. P. Robalo, A. P. S. Teixeira, A. R. Dias, M. F. M. Piedade, M. T. Duarte, *J. Organomet. Chem.* **2001**, *632*, 145–156.
- [22] L. J. Farrugia, *J. Appl. Crystallogr.* **1997**, *30*, 565.
- [23] J. H. Lee, B. S. Yoo, S. W. Lee, *Inorg. Chim. Acta* **2001**, *321*, 75–82.
- [24] M. Hirano, S. Kiyota, M. Imoto, S. Komiya, *Chem. Commun.* **2000**, 1679–1680.
- [25] W. Wenseleers, E. Goovaerts, P. Hepp, M. H. Garcia, M. P. Robalo, A. R. Dias, M. F. M. Piedade, M. T. Duarte, *Chem. Phys. Lett.* **2003**, *367*, 390–397.
- [26] B. J. Coe, C. J. Jones, J. A. McCleverty, D. Bloor, G. Cross, *J. Organomet. Chem.* **1994**, *464*, 225–232.
- [27] M. H. Garcia, J. C. Rodrigues, A. R. Dias, M. F. M. Piedade, M. T. Duarte, M. P. Robalo, N. Lopes, *J. Organomet. Chem.* **2001**, *632*, 133–144.
- [28] H. Meier, R. Petermann, J. Gerold, *Chem. Commun.* **1999**, 977–978.
- [29] J. Luo, J. Hua, J. Qin, J. Chen, Y. Shen, Z. Lu, P. Wang, C. Ye, *Chem. Commun.* **2001**, 171–172.
- [30] A. J. Moore, A. Chesney, M. R. Bryce, A. S. Batsanov, J. F. Kelly, J. A. K. Howard, I. F. Perepichka, D. F. Perepichka, G. Meshulam, G. Berkovic, Z. Kotler, R. Mazor, V. Khodorkovsky, *Eur. J. Org. Chem.* **2001**, 2671–2687.
- [31] J. L. Oudar, D. S. Chemla, *J. Chem. Phys.* **1977**, *66*, 2664–2668.
- [32] A. Willetts, J. E. Rice, D. M. Burland, D. P. Shelton, *J. Chem. Phys.* **1992**, *97*, 7590–7599.
- [33] C. H. Wang, Y. C. Lin, O. Y. Tai, A. K. Y. Jen, *J. Chem. Phys.* **2003**, *119*, 6237–6244.
- [34] B. J. Orr, J. F. Ward, *Mol. Phys.* **1971**, *20*, 513–526.
- [35] A. M. Kelley, *J. Opt. Soc. Am. B: Opt. Phys.* **2002**, *19*, 1890–1900.
- [36] G. Berkovic, G. Meshulam, Z. Kotler, *J. Chem. Phys.* **2000**, *112*, 3997–4003.
- [37] C. H. Wang, *J. Chem. Phys.* **2000**, *112*, 1917–1924.
- [38] D. D. Perrin, W. L. F. Armarego, D. R. Perrin, *Purification of Laboratory Chemicals*, Pergamon Press, New York, **1980**.
- [39] P. Giannoccaro, A. Sacco, *Inorganic Synthesis*, McGraw-Hill Book Company, **1977**, vol. XVII.
- [40] P. E. Hanna, R. E. Gammans, R. D. Schon, M. K. Lee, *J. Med. Chem.* **1980**, *23*, 1038–1044.
- [41] T. van Es, *J. Chem. Soc.* **1965**, 1564.
- [42] L. M. Harwood, C. J. Moody, J. M. Percy, *Experimental Organic Chemistry – Standard and Microscale*, 2nd ed., Blackwell Science Oxford, **1998**.
- [43] A. P. S. Teixeira, PhD Thesis, University of Évora, **2004**.
- [44] A. Altomare, M. C. Burla, M. Camalli, G. L. Cascarano, C. Giacovazzo, A. Guagliardi, A. G. G. Moliterni, G. Polidori, R. Spagna, *J. Appl. Crystallogr.* **1999**, *32*, 115–119.
- [45] G. M. Sheldrick, *SHELXL-97, a program for refining crystal structures* Göttingen, **1997**.
- [46] L. J. Farrugia, *J. Appl. Crystallogr.* **1999**, *32*, 837–838.
- [47] R. W. Terhune, P. D. Maker, C. M. Savage, *Phys. Rev. Lett.* **1965**, *14*, 681–684.
- [48] K. Clays, A. Persoons, *Phys. Rev. Lett.* **1991**, *66*, 2980–2983.
- [49] F. Kajzar, I. Ledoux, J. Zyss, *Phys. Rev. A* **1987**, *36*, 2210–2219.
- [50] D. P. Seccombe, R. P. Tuckett, H. Baumgartel, H. W. Jochims, *Phys. Chem. Chem. Phys.* **1999**, *1*, 773–782.

Received: November 24, 2005
Published Online: April 11, 2006